Makara J. Technol. 23/3 (2019), 111–118
doi: 10.7454/mst.v23i3.3880

A New Synthesized Microalloys Steel ODS of High Amplitude Ultrasonically Irradiation

Marzuki Silalahi[1*], Hanif Abdurrahman Wicaksana[2], Ferhat Aziz[1], Syahfandi Ahda[1], and Mohamad Riza Iskandar[3]

1. PSTBM-BATAN, Puspiptek Serpong Area, Tangerang Selatan 15314, Indonesia
2. Department of Metallurgy, Faculty of Engineering, Universitas Indonesia, Depok 16424, Indonesia
3. Central Facility for Electron Microscopy, RWTH Aachen University, Aachen 52074, Germany

[*]*e-mail: silalahimarzuki@gmail.com*

Abstract

Micropowders of oxide-dispersion-strengthened (ODS) steel have been synthesized using the ultrasonic irradiation method with variations in amplitude. The ultrasonic irradiation process is performed for 50 h at a frequency of 20 kHz with 40%, 50%, and 60% amplitudes in toluene solution. The formation of Fe-Cr microalloys in the preparation of Fe-15Cr-0.5Y_2O_3 powder was analyzed using SEM-EDS, X-ray diffraction (XRD), and TEM-EDS. The percentage of Fe-Cr phase mass fraction of ODS steel micropowder formed during ultrasonic irradiation with 40%:50%:60% amplitude was 12.2%:34.1%:22.1%, with 25.67:77.02:38.51 nm crystallite size. The crystallite size at 50% amplitude was the largest, and the diffusion process of Fe-Cr-Y_2O_3 microparticles was most dominant at 50% amplitude. The Fe and Cr phases are still present when the ODS particles successfully dispersed in the main particle.

Abstrak

Sintesis Baru Paduan Mikro Baja ODS dengan Irradiasi Ultrasonik Amplitudo Tinggi. Serbuk mikro dari baja yang diperkuat dengan dispersi oksida (ODS) telah disintesis menggunakan metode iradiasi ultrasonik dengan variasi amplitudo. Proses iradiasi ultrasonik dilakukan selama 50 jam pada frekuensi 20 kHz dengan amplitudo 40%, 50%, dan 60% dalam larutan toluena. Pembentukan paduan mikro Fe-Cr dalam preparasi serbuk Fe-15Cr-0.5Y2O3 dianalisis menggunakan SEM-EDS (*scanning electron microscopy–energy-dispersive spectroscopy*), difraksi sinar-X (XRD), dan TEM-EDS (*transmission electron microscopy–energy-dispersive spectroscopy*). Persentase fraksi massa fasa Fe-Cr dari serbuk mikro baja ODS yang terbentuk selama iradiasi ultrasonik dengan amplitudo 40%: 50%: 60% adalah 12,2%:34,1%: 22,1%, dengan ukuran kristalit 25,67: 77,02: 38,51 nm. Ukuran kristalit pada amplitudo 50% adalah yang terbesar, dan proses difusi partikel mikro Fe-Cr-Y_2O_3 paling dominan pada amplitudo 50%. Fasa Fe dan Cr masih ada ketika partikel ODS berhasil terdispersi dalam partikel utama.

Keywords: ODS steel, ultrasonic irradiation, high amplitude, microalloying, cavitation

1. Introduction

One of the potential technologies in supplying the world energy demand is advanced nuclear reactors, which can be operated safely and reliably. Therefore, the design of reactor components, such as fission reactor cladding and structural materials, must be tested under extreme conditions with temperatures reaching 700 °C and high irradiation doses. Oxide-dispersion-strengthened (ODS) steels and ferritic/martensitic Fe-Cr alloys are materials that are leading candidates for this application because of its high-temperature strength and high-dimensional stability under irradiation [1],[2]. One of the attractive properties of ODS steel is its swelling resistance caused by radiation; moreover, ODS steel has increased creep strength and is resistant to oxidation/corrosion at high temperatures, when compared with conventional steel [3].

Traditionally, ODS steel is synthesized by mechanical alloying processes, such as ball milling [4]. Although this technique is quite simple, one needs to be careful

when controlling many parameters. Another technique used to synthesize microalloys of steel is the ultrasonication process. Several works reported that the integration of ultrasonication can synthesize microalloys of steel in an easy and efficient manner [5]-[8].

The synthesis of metal alloys using ultrasonic irradiation is a new technique in the formation of microalloys. The chemical effect of this synthesis that occurs in toluene solutions mainly originates from the presence of acoustic cavitation from high-intensity ultrasonic irradiation, resulting in the formation and collapse of bubbles in the liquid. Therefore, the shock wave generated from the explosion of the bubble can cause small particles with large force to collide with each other, resulting in the melting of particles [5].

According to the research conducted by Tzanakis et al. [9], the high intensity of ultrasonic waves will affect the amplitude and intensity of cavitation in a medium [10]. Furthermore, Pokhrel reported that the amplitude and frequency will affect the acoustic pressure acting on particles [11],[12]. On the basis of these previous studies, in the current work, we will present the research results of the synthesis of Fe-Cr microalloy using ultrasonic irradiation with variations in amplitude. The details of the analysis performed by X-ray diffraction (XRD), scanning electron microscopy–energy-dispersive spectroscopy (SEM-EDS), and transmission electron microscopy (TEM) will also be presented.

2. Experiment

In this work, Fe, Cr, and yttrium oxide Y_2O_3 powders (made by Aldrich) with a purity of 99.9% have been used. In addition, toluene solution with a purity of 90% (a product of Aldrich) is used as powder medium in ultrasonic treatment. First, all materials are weighted with a percentage ratio of Fe:Cr:Y_2O_3 of 84.5:15:0.5.

Afterward, these powders were mixed with the toluene solution [5],[8]. Then, ultrasonication was performed at a constant frequency of 20 kHz for 50 h with variations in amplitude of 40%, 50%, and 60% (see Table 1). For the ultrasonic treatments, the Ultrasonic Horn type Autotune series, VCX 750 model TI was used.

After synthesis, the phase formation of the samples was investigated by means of XRD from PANalytical Empyrean CuKα. The acquired XRD patterns were analyzed using the Rietveld technique with the help of the HighScore Plus software.

To determine the particle sizes of the samples during the ultrasonic treatments, microanalysis was conducted using the SEM Jeol JSM-6510LA equipped with EDS detector from EDAX. The details of the internal structure of the powder were investigated by means of

Table 1. Summary of the Treatment of Samples

Sample	Treatment	Time (h)	Frequency (kHz)	Amplitude (%)
A	Mixing on mortar	0.25	–	–
B	Ultrasonic irradiation on toluene medium	50	20	40
C	Ultrasonic irradiation on toluene medium	50	20	50
D	Ultrasonic irradiation on toluene medium	50	20	60

TEM performed on a thermionic emission Tecnai F20 operated at 200 kV and equipped with EDS detector from EDAX. The DiffTools script package for Digital Micrograph™ was used to analyze the electron diffraction patterns [13].

3. Results and Discussion

Figure 1 shows the SEM-BSE micrographs with the corresponding EDS spectra of the samples. The BSE images reveal no significant differences in the size and morphology of all particles produced by ultrasonication. These particles are approximately 2 μm to 10 μm in size. Most particles have a spherical form, which indicates that ultrasonication has successfully prevented the particle from being granulated. EDS analysis revealed the phase presence on three synthesized samples. From selected areas (the points shown in Figure 1, such as point 015 of Figure 1(a), point 002 of Figure 1(b), and point 003 of Figure 1(c)) on these samples, a particle exhibits (after ultrasonication) peaks that consist of Fe, Cr, and Y_2O_3, indicating the Fe-Cr alloys. Semiquantitatively, Figure 1(a) shows the composition of Fe = 88.03%, Cr = 6.59%, and Y = 3.62% at point 015. Figure 1(b) shows the composition of Fe = 43% and Cr = 57% at point 002. The composition value of Figure 1(b) is determined to be so close that it shows that the combination of Fe and Cr has formed a new Fe-Cr phase. This illustrates that the process of ultrasonication has resulted in the integration of particles. Then, the same effect occurred in sample D at an amplitude of 60%. Figure 1(c) shows the composition of Fe = 93.38%, Cr = 3.92, and Y = 2.70% at point 003. In addition, in Figure 1(b), the EDS spectra clearly show a higher concentration of Cr on sample C than that of the two other samples.

The existence of these phases can also be observed in the XRD patterns of the four samples presented in Figure 2 at diffraction angles of 40° to 120°. Meanwhile, angles below 40° do not have a dominant peak. Sample A shows the highest XRD peaks.

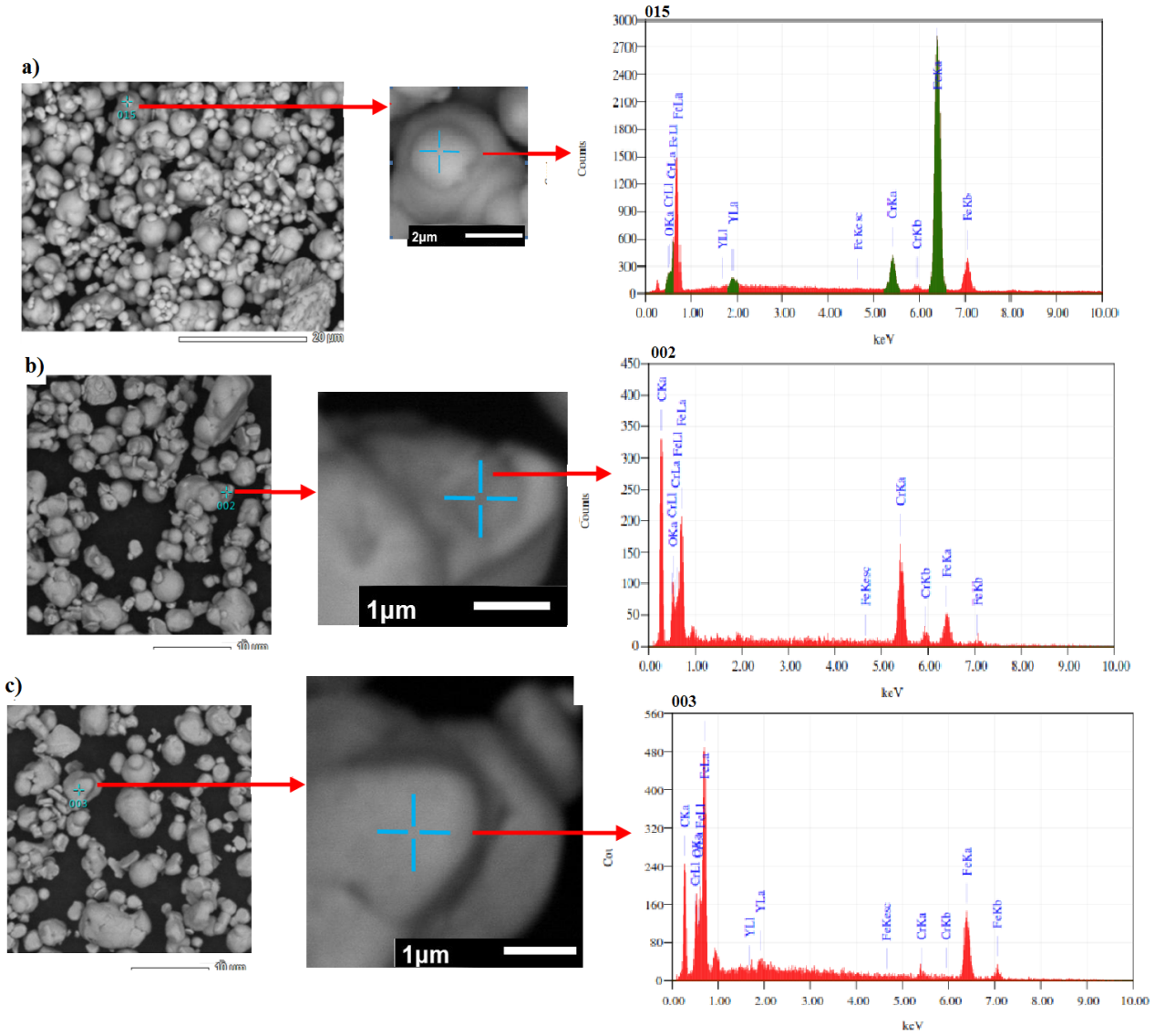

Figure 1. SEM-BSE Images and EDS Spectra of the Synthesized Samples with the Ultrasonification Amplitudes of (a) 40%, (b) 50% [7], and (c) 60%

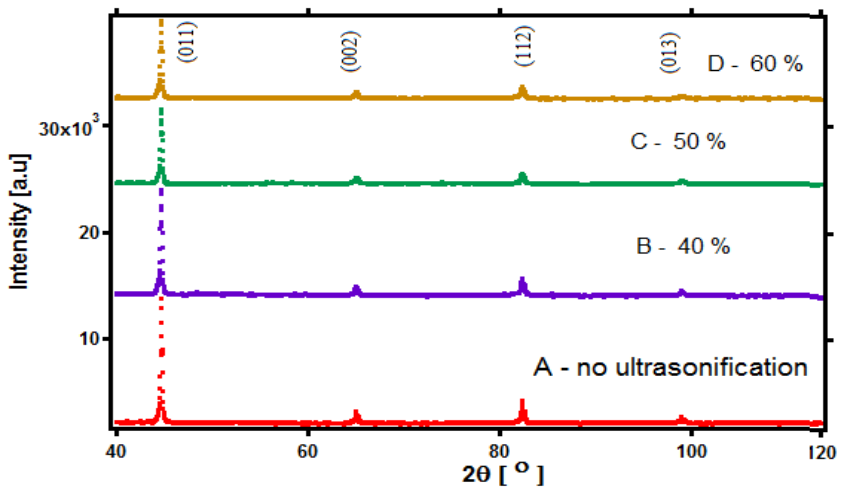

Figure 2. XRD Pattern for (a) A, Mortar, 0%, (b) B, 40%, (c) C, 50%, and (d) D, 60% of Amplitude Intensity

However, for samples B, C, and D after synthesis, a decrease in the lowest peak can be observed. This finding can be attributed to the formation of a new phase (Fe-Cr) or a change in the content of the basic materials. Therefore, the refinement process was conducted using the Rietveld method with the help of the HighScore Plus program to analyze the crystal structure from the synthesis results, as shown in Figures 3 and 4.

First, we analyzed the results of the refinement process of sample A, which did not involve ultrasonic irradiation. Of course, no new phase was formed and only the XRD patterns of the basic materials were observed.

As shown in Figure 3, as a result of the refinement process, the total calculation peaks at the angular ranges of 43.5° to 45.5° and 64.0° to 66.0° are close to the observation peak. The statistical errors of the weight profile R factor (Rwp) and expected profile R factor (Rp) have values of 2.31% and 2.07%, respectively. These statistical errors are consistent with the refinement process because it is less than 10%. Compared with the refinement of $PbSO_4$ conducted by R.J. Hill, the statistical errors were approximately 7.14% to 10.08% [14]. Of course, this refinement process is feasible and good enough to continue with samples using ultrasonic treatment. Figure 3 shows the visual comparison of the blue peak representing the Fe phase, which is highly dominant, and the green peak representing the Cr phase, which is related to the content of each phase itself. The contents of the Fe and Cr phases are 84.7% and 15.3%, respectively, and are close to the basic composition (85% and 15%, respectively), which is consistent with the refinement process.

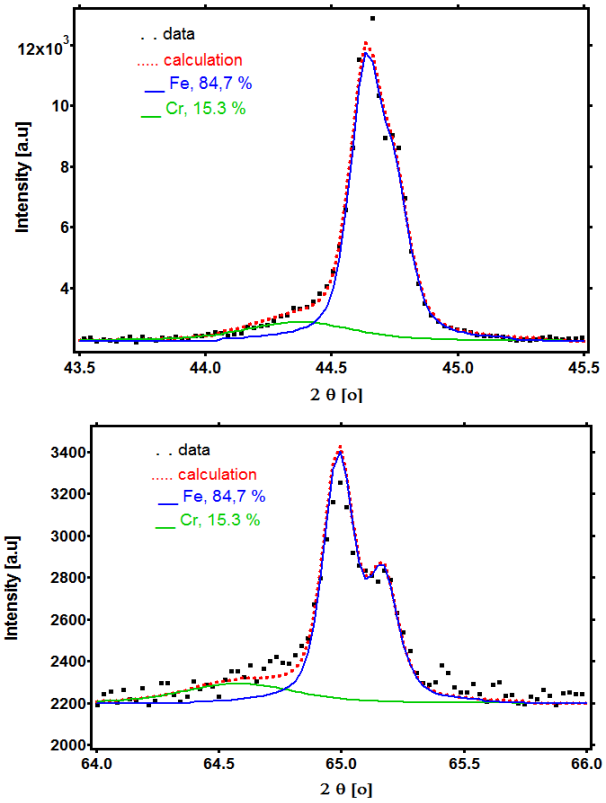

Figure 3. Refinement XRD Profile Curve of Sample A with no Ultrasonic Treatment. The Black dot Represents the Observation Data, whereas the Red dot Represents the Calculation Data. The Blue Line Represents the Fe Phase and the Green Line Represents the Cr Phase, which are the Output of the Refinement Process

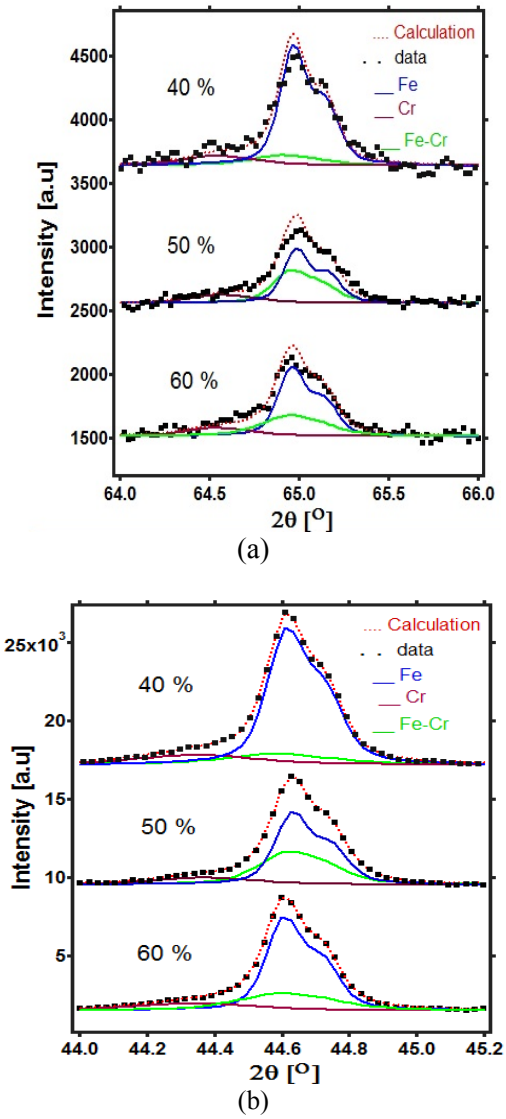

Figure 4. Refinement Curve of the Ultrasonic Treatment of the Samples for 50 h with Amplitude Variations of 40% (Sample B), 50% (Sample C), and 60% (Sample D) at 2θ Angles of (a) 44.0° to 46.2° and (b) 64.0° to 66.0°. The Black Dot Represents the Experimental Intensity Data. Meanwhile, the Refinement Process Results are Displayed with Total Intensity (Labeled Calculation, Red Dot), Fe Phase (Blue Line), Cr Phase (Red Line), and Fe-Cr Phase (Green Line)

As mentioned previously, this refinement process revealed that the crystal structures for Fe and Cr have the Im-3 m (cubic) and I4/mmm (tetragonal) space groups, respectively. The refinement results also indicate lattice parameters, as shown in Table 2. The Fe crystal system is cubic, whereas the Cr crystal system is close to cubic because the lattice parameter of a is close to c, as indicated by the refinement results also shown in Table 2.

The obtained data of Fe and Cr were used as the input in the refinement process of samples B, C, and D, which have been treated with ultrasonic irradiation at the same time and amplitude variations. Figure 4 shows the results of the refinement process for each phase, i.e., Fe (Im-3 m space group), Cr (I4/mmm space group), and Fe-Cr (Im-3 m space group). With the space group of the three phases being nearly the same as a cubic crystal system, the index to represent each plane is also the same, as shown in Figure 2.

The ultrasonic irradiation treatment of samples B, C, and D for 50 h with varying amplitudes can be expected to form Fe-Cr compounds. Qualitatively, the content of the Fe-Cr phase can be represented by the low–high peaks, as shown in Figure 4. Sample C has the highest peak compared with samples B and D. However, quantitative XRD profile analysis of samples B, C, and D has been conducted using the Rietveld method with the help of the HighScore Plus program, as shown in Table 3.

The percentages of the phases in each sample are shown in Table 3. The results of the refinement process show that sample A does not contain Fe-Cr (as mentioned previously). Meanwhile, the highest Fe-Cr content of 34.1% with the lowest lattice parameter of 2.8673 Å was observed in sample C.

During the synthesis process using ultrasonic irradiation techniques with various amplitude forces, of course, crystal defects can occur because of the formation of polycrystalline aggregations. This has an effect on the size of the crystallite produced, which can lead to the broadening–narrowing of the XRD peak. The size and strain can also affect the broadening of the peak and can be estimated using Williamson–Hall's analysis method as a function of the broadening peak width and peak position 2θ [15],[16].

Tabel 2. Lattice Parameters of the Fe and Cr Crystal Structures in Sample A (No Ultrasonic Treatment), which were the Result of the Refinement Process

Phase	Lattice Parameters (Å)
Fe	a = b = c = 2.8658
Cr	a = b = 2.8839
	c = 2.8854

Table 3. Results of the Refinement Process with Lattice Parameters and the Content of Fe-Cr Formed in Each Sample Treated Using Ultrasonic Irradiation

Samples	Lattice parameter (Å)	Crystallite size [nm]	Content [wt%]		
	Fe-Cr	Fe-Cr	Fe	Cr	Fe-Cr
B	a = b = c = 2.870(1)	25.67	74.9	12.9	12.2
C	a = b = c = 2.8673(5)	77.02	54.2	11.8	34.1
D	a = b = c = 2.8675(5)	38.51	65.4	12.5	22.1

Through this approach, the Williamson–Hall plot is formulated with straight-line functions using the equation $\beta\cos\theta = k\lambda/d + 4\varepsilon(\sin\theta)$. The results of the refinement process in this study are illustrated in Figure 5, where d is the crystallite size, (ε) is the elastic strain, β is the full width at half maximum (FWHM), and K is the Scherrer constant (a rather arbitrary value, which falls in the range of 0.87–1.0; we usually assume that K = 1). The determination of the FWHM from the XRD intensity profile was first corrected with standard silicon samples, as conducted by Engkir [17]. Thus, the size of the crystallite is obtained by extrapolation using the aforementioned equation.

The extrapolation of the equation to the *Y*-axis, as shown in Figure 5, enables the calculation of the value of the crystallite size under each amplitude, as specified in Table 3. The largest crystallite size, i.e., 77.02 nm, is observed in samples with an amplitude of 50%. This finding indicates that the reaction rate or diffusion process is fast at an amplitude of 50% in toluene solution.

To observe the granules of the samples that underwent ultrasonic treatment, morpholgic images were taken using TEM. Figure 7 shows the TEM brightfield images of the particles from sample D. Particles with irregular shape and size of 2 μm is shown in Figure 7(a). Moreover, some particles show a strong diffraction contrast, which indicates that some defects formed on the particles. These defects were probably induced by the size of ODS particles that formed after mechanical alloying. This indication can be confirmed by the detailed information obtained from higher magnification image of other particles, as shown in Figure 7(b). The TEM brightfield images revealed some nanoparticles, which are probably ODS particles, with the size of approximately 20 nm, dispersed on one large grain. This size is close to the size of crystallite particles in Fe-Cr (i.e., 38 nm, from the results of XRD analysis) observed through TEM analysis. Further analysis by means of high-resolution TEM and EDS could be performed to identify the origin of these particles.

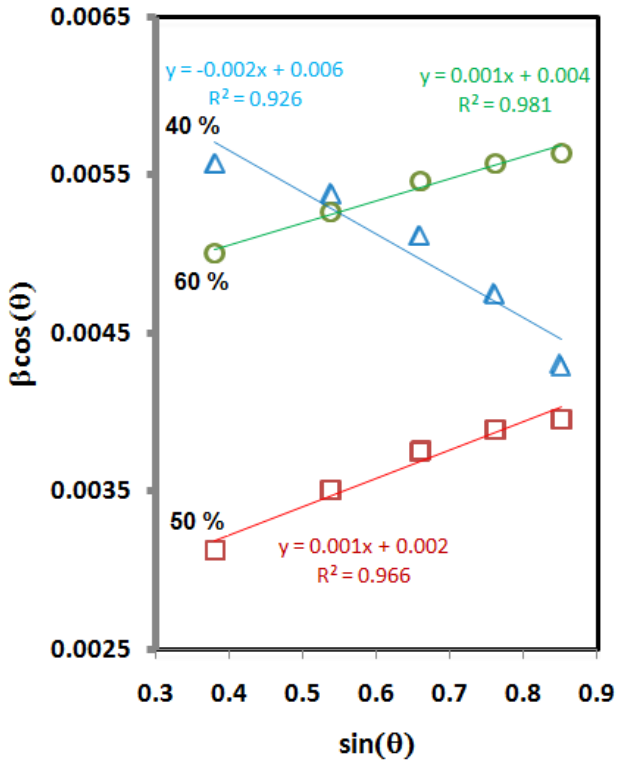

Figure 5. Williamson–Hall Plot of the Results of the Refinement Process of the Fe-Cr Phase and Straight-line Equations for Each Sample with Ultrasonic Amplitudes of 40%, 50%, and 60%, where βcos(θ) = Y and sin (θ) = x

The size of the dispersed particles is relatively small to identify by XRD analysis. Thus, electron diffraction and energy-dispersive X-ray analyses of some selected particles were conducted to identify the phase presence locally. The selective area electron diffraction (SAED) pattern taken from one area containing some particles is shown in Figure 8(a). The pattern consists of incomplete rings, which indicate that the size of the particles is quite large. Most of the primary reflections can be identified as cubic Fe and Cr. Some of minor reflections can be identified as oxide particles. Additional information from the TEM-EDS spectrum obtained from one selected area verified the SAED pattern. The strong signals of Fe and O indicate that localized Fe and Cr phases are still present in ODS particles successfully dispersed in the main particle. Although XRD indicates the formation of the Fe-Cr phase, it does not homogenously distribute as TEM analysis of the selected area did not reveal the presence of the Fe-Cr phase.

Defects or surface defects caused by surface deformation will result in new nucleation or cavitation formation [18], resulting in new cavitation and microjet, which will re-deform the surface to make the surface of the particles cleaner [11] and to further increase the surface reactivity of the particles. The ultrasonic waves applied to the toluene solution will move the particles with the density and strain of longitudinal waves [12] and lead to the occurrence of similar particle collisions between Fe or Cr particles, which is called cohesive particle collisions [5], or between different particles, i.e.,

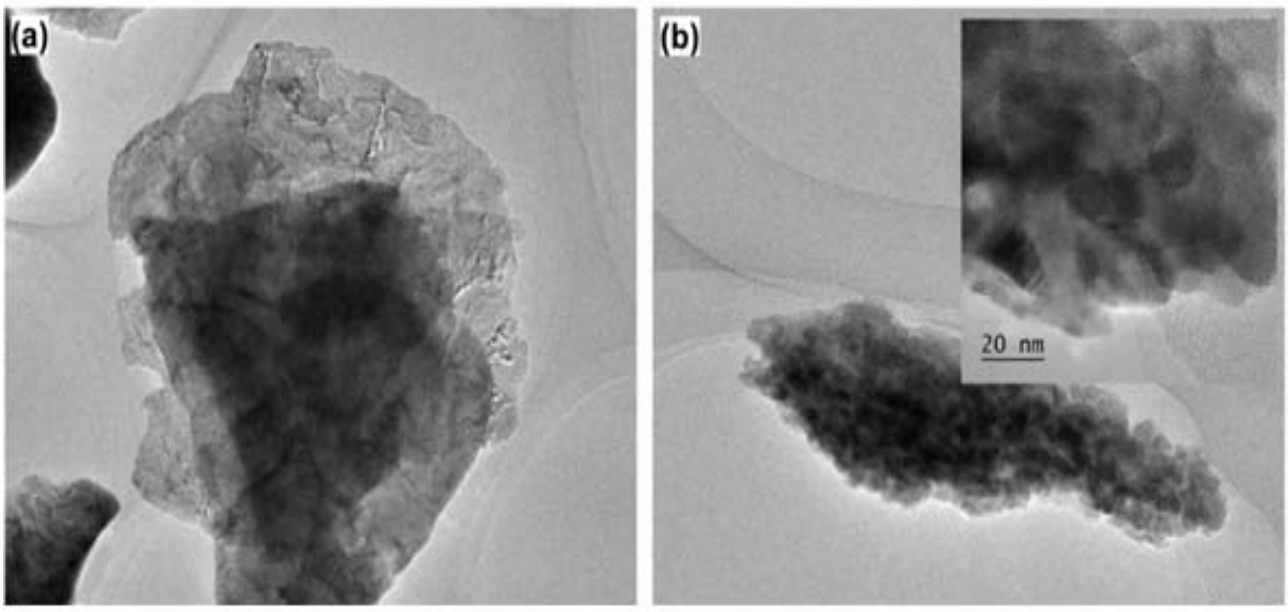

Figure 6. TEM Brightfield Images of Sample D, i.e., Fe-Cr ultrasonically Treated with an Amplitude of 60%: (a) One Particle Contains Local Defects and (b) Nanoparticles Dispersed in the Particle Matrix

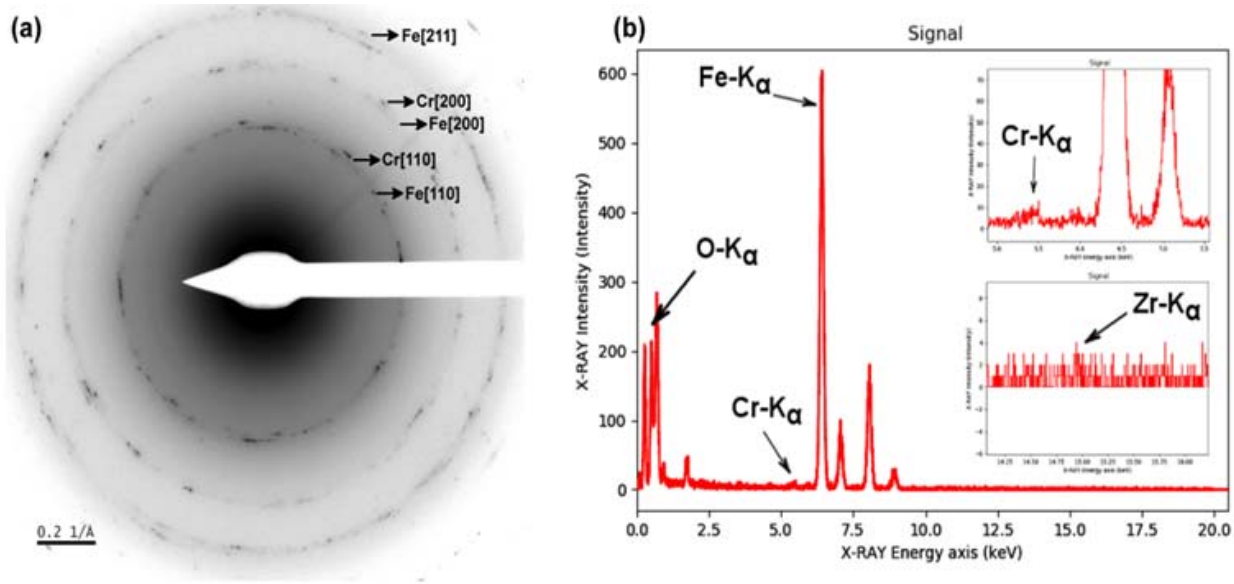

Figure 7. (a) SAED Pattern Taken from One Area Containing some Particles and (b) TEM-EDS Spectrum Obtained from one Selected Area

Fe with Cr, Y_2O_3 with Fe, or Y_2O_3 with Cr. If the collision is perfect, then friction will occur between particles and cause the reduction in the grain size. In case of imperfect collision [19], union of particles called powder agglomeration will occur. Previous studies reported the incorporation of similar particles due to the collision of particles during the ultrasonication process [19]. In this study, the oxide phase does not form on powder samples A, B, C, and D because toluene is incompatible with strong oxidizers; thus, it is not readily oxidized [20]. The higher the viscosity of the liquid is, the harder it is to form cavitation. Toluene has a specific gravity of 0.886 m·g/v, whereas water has a specific gravity of 1 m·g/v [21,22]. Hence, cavitation easily occurs in toluene media.

4. Conclusion

Microalloy Fe-Cr ODS synthesis using the ultrasonic method was successfully conducted. The percentage of the maximum mass fraction of the micropowder Fe-Cr phase from ODS steel formed through ultrasonic irradiation at 50% amplitude with lattice parameter of 2.8673 A is 34.1%. The crystallite size at 50% amplitude is the largest. Ultrasonication of Fe-Cr-Y_2O_3 ODS steels in toluene solution does not produce an oxide phase.

Acknowledgement

The authors would like to thank the Head of PSTBM BATAN, along with the staff so that this research can be completed. This research was funded by DIPA PSTBM BATAN. The authors would like to thank Drs. Bambang Sugeng who has assisted in taking XRD diffraction pattern data.

References

[1] M. Yurechko, C. Schroer, O. Wedemeyer, A. Skrypnik, J. Konys. Nucl. Eng. Des. 280 (2015) 686.
[2] I. Hilger, X. Boulnat, J. Hoffmann, C.Testani, F. Bergner, Y. De Carlan, F. Ferraro, A. Ulbricht, J. Nucl. Mater.472 (2016) 206.
[3] L.L. Hsiung, M.J. Fluss, S.J. Tumey, B.W. Choi, Y. Serruys, F. Willaime, A. Kimura, Phys. Rev. B 82 (2010) 184103.
[4] S. Li, Z. Zhou, J. Jang, M. Wang, H. Hu, H. Sun, L. Zou, G. Zhang, L. Zhang, J. Nucl. Mater. 455/1-3 (2014) 194.
[5] M. Silalahi, A. Dimyati, S. Harjanto, P. Untoro, B. Suharno, Int. J. Technol. 5/2 (2014) 169.
[6] M. Silalahi, P. Untoro, B. Suharno, S. Harjanto, Jusami 15/3 (2014) 123.
[7] M. Silalahi, P. Untoro, B. Suharno, S. Harjanto, Majalah Metalurgi 29/2 (2014) 171.
[8] M. Silalahi, H.A. Wicaksana, B. Sugeng, A. Dimiyati, B. Suharno, Prosiding Seminar Nasional Teknologi Energi Nuklir, 1 (2016) 345.
[9] I. Tzanakis, G.S.B. Lebon, D.G. Eskin, K. Pericleous, Mater. Des.90 (2016) 979.
[10] T. Prozorov, R. Prozorov, and K. S. Suslick, J. Am. Chem. Soc. 126/43 (2004) 13890.
[11] N. Pokhrel, P.K. Vabbina, N. Pala, Sonochem. 29 (2016) 104.
[12] L. Pascal, H. Guillaume, Springer (www.springer.com), 2011, [https://epdf.pub/queue/bone-quantitative-ultrasound.html].
[13] D.R.G. Mitchell, Microsc. Res. Tech., 71 (2008) 588.
[14] R. J. Hill, J. Appl. Cryst. 25 (1992) 589.

[15] Y.T. Prabhu, K.V. Rao, V.S.S. Kumar, B.S. Kumari, World J. Nano Sci. Eng. 04/01 (2014) 21.
[16] S. Ahda, S. Misfadhila, P. Parikin, T.Y.S.P. Putra, IOP Conf. Ser. Mater. Sci. Eng., 176/1 (2017) 012048.
[17] E. Sukirman, Y. Sarwanto. Jusami 15/2 (2014) 63.
[18] T.Y. Wu, N. Guo, C.Y. The, J.X.W. Hay, Theory and Fundamentals of Ultrasound in Advances in Ultrasound Technology for Environmental Remediation, Springer Briefs in Green Chemistry for Sustainability, 2013, p. 5-11.
[19] S.J. Doktycz, K.S. Suslick, Science 247/ 4946 (1990) 1067.
[20] Q. Zhao, L. Yu, Y. Liu, H. Li, Adv. Powder Technol. 26/6 (2015) 1578.
[21] B. Saleh, A.E. El-deen, S.M. Ahmed, J. Eng. Sci. 39/2 (2011) 327.
[22] Met Prep Ltd, Conducto-Mount 2 Material Safety Data Sheet, 2015. [*Sciencelab.com*].